# The Analysis of the Polaroid Optocoupler Mechanical-electrical Sensor

Ioan Marcel CIURUŞ, Mihai DIMIAN, Adrian GRAUR
*Stefan cel Mare University of Suceava, 720229, Romania*
*marcelciurus@usv.ro*

***Abstract*—This paper presents the results of the analysis of Polaroid optocoupler mechanical-electrical sensor static characteristics. Our paper achieves analysis on distance adjustment Polaroid optocouplers of LED-photoresistor and LED-phototransistor types. These optocouplers analysis was performed in two distinct cases by using 0.2 mm and 0.7 mm thick Polaroid filters. At present, this Polaroid optocoupler mechanical-electrical sensor is only a prototype.**

***Index Terms*—Mechanical-electrical sensor, Optical polarization, Optoelectronics, Polaroid optocoupler.**

## I. Introduction

The development of modern industrial activities represents a real challenge for the 'science of measurement'. Therefore, the diversification of the nature of interactions between the mechanical components of different machines with the exterior medium or/and of the physical processes standing at the basis of their functioning has determined the intensification of the research within the sensors field [1]. The obtaining of new sensors and the analysis of their characteristics and optimization, allow the accurate measurement of a vast range of physical quantities whose measurement is indispensable for the new technological processes [2]-[4].

In this paper, it is presented a part of our research in the field. This research is centred upon designing, analyzing and optimizing optical sensors of the PO Polaroid optocoupler. Our attention has been focused on optical sensors, since direct photoelectrical conversions aren't influenced by electromagnetic perturbations [4].

PO Sensor is an optocoupler, where a system of two Polaroid filters is introduced on the way of the light beam performing the optical coupling. This system of filters allows the mechanical modification of the optocoupler output parameters. At present, this sensor is only a prototype.

Although the PO sensor is an analogue device, the digital optical encoders can be replaced by using an analogue-to-digital converter.

As for digital optical encoders, PO sensors present the following advantages: they can be much better miniaturized, their resolution isn't limited to the density of the opaque and transparent areas, there isn't any information loss in case of high speeds or voltage falls, they can simultaneously transform both rotation and translation movements into electrical signals.

## II. Sensor Description

The PO sensor is an optoelectronical device made up of: light source, photosensitive element, assembly of Polaroid filters (A-analyzer and P-polarizer) and a mechanical system allowing the components axial assemblage, as well as their startup, Fig. 1, [5].

The Polaroid polarizer filter (P) is fixed at the optical output of the transmitter module ($T_x$) and the Polaroid analyzer (A) filter is fixed at the optical entrance of the receiver module ($R_x$).

Optocoupler mechanical system is designed to enable modules ($T_x$) and ($R_x$) to perform axial movements of rotation and/or translation one towards the other.

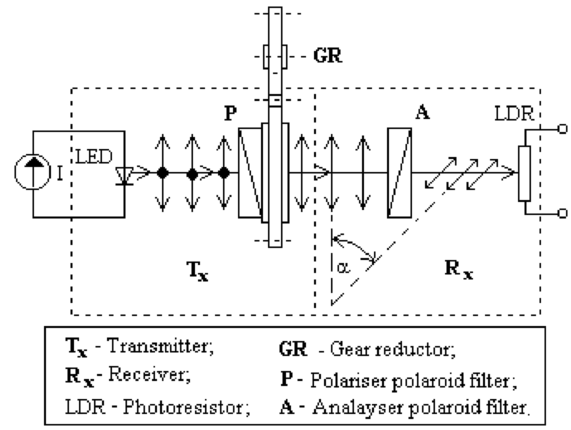


Fig. 1. The diagram of the LED–photoresistor PO sensor.

This sensor can be designed in two ways: PO sensor with distance adjustment and PO sensor without distance adjustment, Fig. 2.

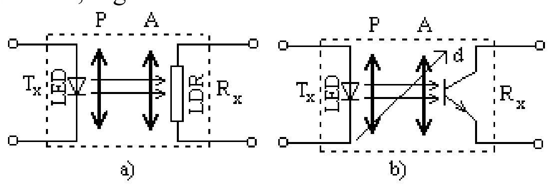


Fig. 2. a) LED–photoresistor PO sensor without distance adjustment; b) LED–phototransistor PO sensor with distance adjustment.

The main characteristic of the PO sensor without distance adjustment consists in the possibility to modify the intensity of the electrical current at the output of the photosensitive element as a result of the processes of in-line polarization and re-orientation of the polarizing plan of the light beam performing the optical coupling.

If the PO sensor is fitted with distance adjustment, then the sensor output electrical current can be also modified by the variation of the distance between ($T_x$) and ($R_x$) modules.

Digital Object Identifier 10.4316/AECE.2010.04005

## III. EXPERIMENTAL RESULTS

The analyzed LED–photoresistor and LED–phototransistor sensors belong to the category of the PO sensors with distance adjustment.

They use as a light source, a super bright white LED of 10.4 cd intensity for a 19 mA current, on the direction of the longitudinal axis.

The experimental determinations have been performed on two sets of 0.2 mm and 0.7 mm thick filters.

The photosensitive element of the LED-phototransistor PO sensors is a BPV 11 Silicon NPN Phototransistor. It requires an open base circuit, having a 18 V emitter-collector voltage.

This sensor transfer experimental characteristics families, $I_C=I_C(\alpha)_{d=const.}$ and $I_C=I_C(d)_{\alpha=const}$, are plotted by dots in Figures 3 and 4, for 0.7 mm filters, and in Figures 5 and 6, for the set of 0.2 mm filters [6], [7].

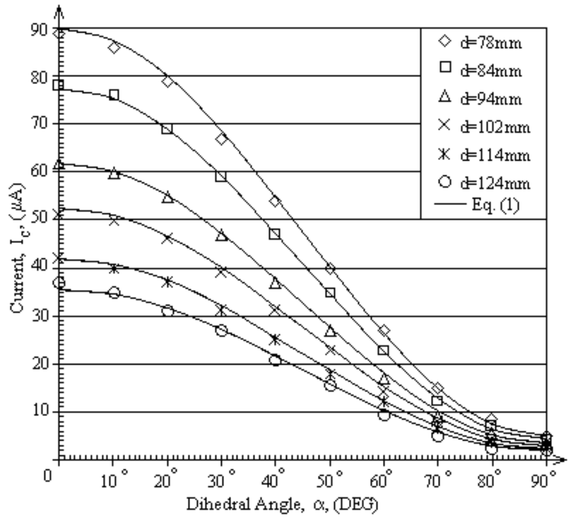


Fig. 3. Graphical representation of the experimental and theoretical characteristics families $I_C=I_C(\alpha)_{d=const.}$ of the LED–phototransistor PO sensor, in the case of filters of 0.7mm.

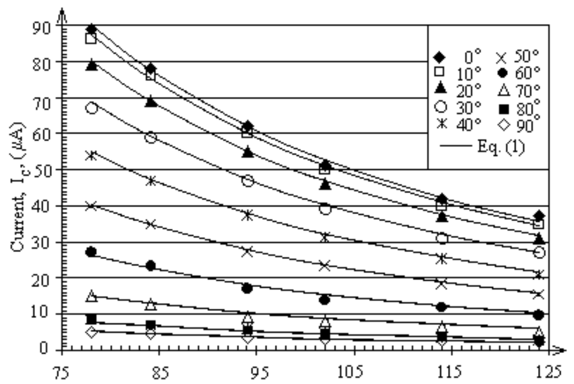


Fig. 4. Graphical representation of the experimental and the theoretical characteristics' families $I_C=I_C(d)_{\alpha=const.}$ of the LED–phototransistor PO sensor, in the case of 0.7 mm filters.

These characteristics show the dependence of the photoresistor output current ($I_C$) on the dihedral angle ($\alpha$), between the polarizing plans of the Polaroid filters (P) and (A), when the distance between modules ($T_x$) and ($R_x$) is constant, in Figures 3 and 5. It also shows the way in which this current is modified at the same time with the variation of the distance (d) between modules ($T_x$) and ($R_x$) when angle ($\alpha$) is maintained constant, in Figures 4 and 6.

In the case of the LED-photoresistor PO sensors, we used a LDR07 photoresistor as the photosensitive element. Its supplying voltage is V = 3 V.

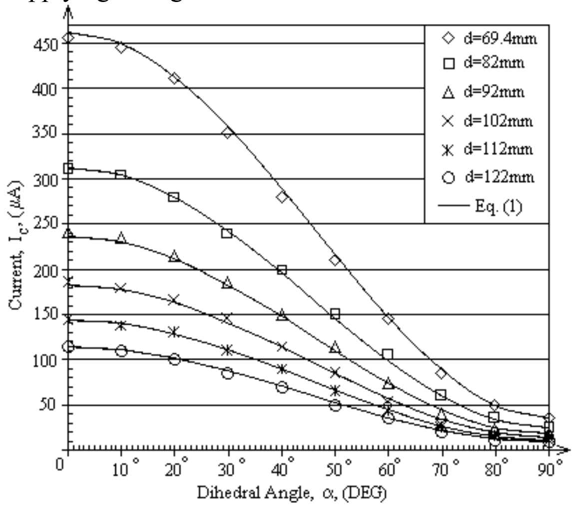


Fig. 5. Graphical representation of the experimental and theoretical characteristics' families $I_C=I_C(\alpha)_{d=const.}$ of the LED–phototransistor PO sensor, in the case of 0.2 mm filters.

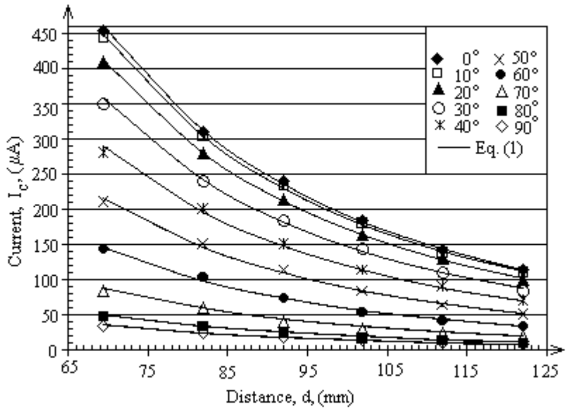


Fig. 6. Graphical representation of the experimental and theoretical characteristics families $I_C=I_C(d)_{\alpha=const.}$ of the LED–phototransistor PO sensor, in the case of 0.2 mm filters.

The experimental characteristics families $I_R=I_R(\alpha)_{d=const.}$ and $I_R=I_R(d)_{\alpha=const.}$ of the LED–photoresistor PO sensor are presented in Figures 7 and 8, for 0.7 mm filters and in Figures 9 and 10, for the set of 0.2 mm filters [7].

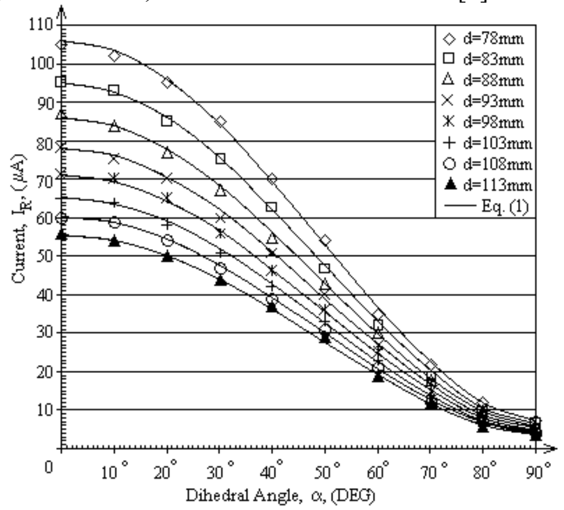


Fig. 7. Graphical representation of the experimental and theoretical characteristics families $I_R=I_R(\alpha)_{d=const.}$ of the LED–photoresistor PO sensor, in the case of 0.7 mm filters.

These characteristics show the dependence of the LED–photoresistor PO sensor output current ($I_R$) on the angle

($\alpha$), when distance (d) is constant, in Figures 7 and 8, as well as the way in which this current is modified at the same time with the variation of the distance (d) between modules ($T_x$) and ($R_x$), when angle ($\alpha$) is maintained constant, in Figures 9 and 10.

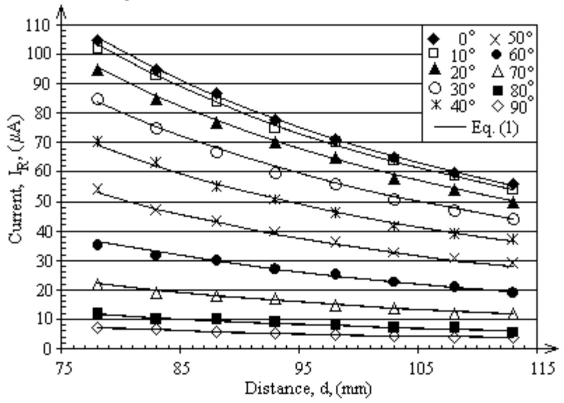


Fig. 8. Graphical representation of the experimental and theoretical characteristics families $I_R=I_R(d)_{\alpha=const.}$ of the LED–photoresistor PO sensor, in the case of 0.7 mm filters.

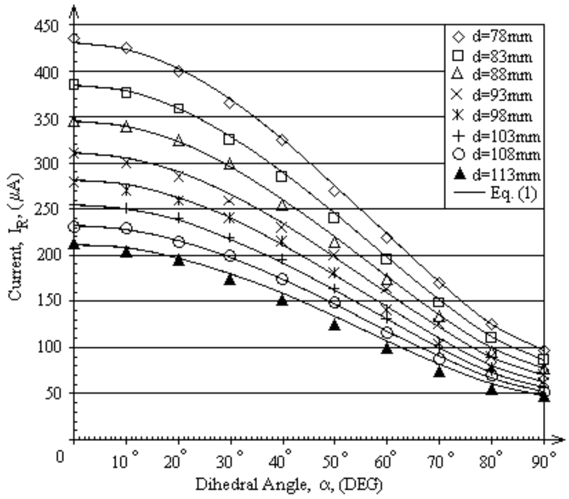


Fig. 9. Graphical representation of the experimental and the theoretical characteristics families $I_R=I_R(\alpha)_{d=const.}$ of the LED–photoresistor PO sensor, in case of 0.2 mm filters.

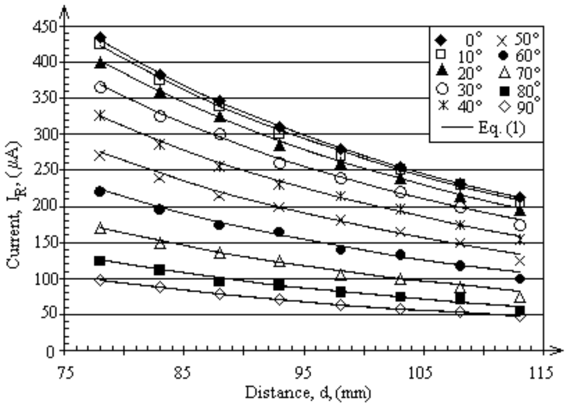


Fig. 10. Graphical representation of the experimental and the theoretical characteristics families $I_R=I_R(\alpha)_{d=const.}$ of the LED–photoresistor PO sensor, in case of 0.2 mm filters.

From Figures 3-10, it can be noticed that the characteristics families $I=I(\alpha,d)$ of LED-phototransistor and LED-photoresistor PO sensors are alike.

These characteristics mathematic expression is given by (1), [7].

$$I = k \cdot \frac{\cos^{2a}\alpha + T}{d^{2a}} \tag{1}$$

where:

- k - optocoupler specific proportionality constant;
- T - represents the transmitting factor of the light beam through the optocoupler optical system, in case of extinction ($\alpha$ = 90°);
- a - the photosensitive element specific parameter. It depends on the form of the light characteristic $I=I(E_v)_{V=const.}$ of the photosensitive element, in its operating point area. This parameter is constant (a≤1), for 0.7 mm filters and in poor lighting conditions. At more intense illuminations, the case of filters of 0.2mm, it depends on the distance (d) between modules ($T_x$) and ($R_x$), Table I.

The empirical values of parameters T, k and a, in the case of the two types of PO sensors, are given in Table I [6], [8].

TABLE I. THE VALUES OF THE PO SENSOR PARAMETERS T, K AND a, IN THE CASE OF 0.7 mm AND 0.2 mm POLAROID FILTERS.

| Constants | PO Sensor | | | |
|---|---|---|---|---|
| | LED-photoresistor | | LED-phototransistor | |
| | 0.7mm | 0.2 mm | 0.7mm | 0.2 mm |
| T | 0.073 | 0.292 | 0.066 | 0.084 |
| a | 0.87 | $0.66 + 5.7\cdot10^{-4}mm^{-1}\cdot d$ | 1 | $0.93 + 5.9\cdot10^{-4}mm^{-1}\cdot d$ |
| k ($mA\cdot mm^{2a}$) | 193.4 | 151.3 | 516 | 1,586.7 |

In Figures 3-10, the theoretical characteristics families of PO sensor are represented by a continuous line, (1).

## IV. PO SENSORS ANALYSIS

PO sensors are non-linear devices (1). This non-linearity is caused by the non-linear dependence of the luminous lighting ($E_v$) of the photoelement on ($\alpha$) angle between the polarizing plans of the Polaroid filters and the distance (d) between modules ($T_x$) and ($R_x$). Consequently, the linearity of the photodiodes light characteristic does not present an advantage in designing PO sensors. In this case, it is preferable to use some photoelements with an increased light sensitivity, as photoresistors and phototransistors, even though their light characteristics are non-linear.

Since PO sensors characteristics are non-linear, their sensitivity is not the same on the whole measurement field. By differentiating (1), we obtained the variation laws of the sensors sensitivity, depending on the position parameters ($\alpha$) and (d):

$$dI = \frac{\partial I}{\partial \alpha}\cdot d\alpha + \frac{\partial I}{\partial d}\cdot dd = S_\alpha \cdot d\alpha + S_d \cdot dd \tag{2}$$

where $S_\alpha$ represents the sensor local angular sensitivity, and $S_d$ is the sensor local linear sensitivity.

In the case of 0.7 mm filters and constant (a) parameter being, PO sensors angular and linear sensitivities are:

$$S_\alpha = -\frac{2a\cdot k}{d^{2a}}\cdot \sin\alpha \cdot \cos^{2a-1}\alpha \tag{3}$$

$$S_d = -\frac{2a\cdot k}{d^{2a+1}}\cdot\left(\cos^{2a}\alpha + T\right) \tag{4}$$

Equation (4) is not true, in the case of 0.2 mm filters. In this case, a = a(d), the linear sensitivity of PO sensors is given by (5):

$$S_d = \frac{2k}{d^2}\cdot\left[B\cdot\cos^{2a}\alpha\cdot\ln(\cos\alpha) - \left(\cos^{2a}\alpha + T\right)\cdot\left(\frac{a}{d} + B\cdot\ln d\right)\right] \quad (5)$$

where B = 5.9·10$^{-4}$ mm, in the case of the LED-phototransistor PO sensor, and B = 5.7·10$^{-4}$ mm, in the case of the LED-photoresistor PO sensor, Table I.

To compare the sensitivities of the two types of PO sensors, in the case of the two sets of Polaroid filters, their sensitivity analysis is performed depending on the relative angular and linear sensitivities:

$$S_{\alpha r} = \frac{S_\alpha}{S_{\alpha\, max.}} \quad (6)$$

$$S_{dr} = \frac{S_d}{S_{d\, max}}. \quad (7)$$

where $S_{\alpha max.}$ represents the maximum value of the angular sensitivity, when d = const. and $S_{dmax}$ is the maximum linear sensitivity, when $\alpha$ = const.

Fig. 11 presents the characteristics $S_{\alpha s} = S_{\alpha r}(\alpha)_{d=const.}$ of the two types of PO sensors, for the sets of 0.2 mm and 0.7mm filters. These characteristics show the dependence of the relative angular sensitivity on angle ($\alpha$), when the distance between modules ($T_x$) and ($R_x$) is constant.

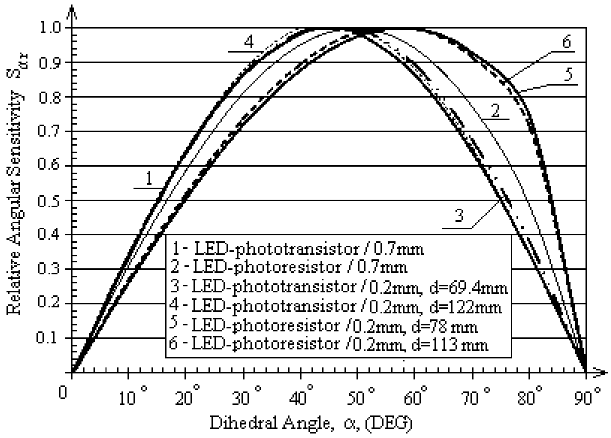


Fig. 11. Graphical representation of the characteristics $S_\alpha = S_{\alpha r}(\alpha)_{d=const.}$ of the LED–phototransistor and LED–photoresistor PO sensor, (3).

The maximum values expressed in (μA/DEG), of the angular sensitivity module of the two types of PO sensors, in the case of the two sets of filters, corresponding to the extreme values of distance (d), are represented in Table II.

TABLE II. THE MAXIMUM VALUES EXPRESSED IN (μA/DEG), OF THE ANGULAR SENSITIVITY MODULE OF THE LED-PHOTOTRANSISTOR AND LED-PHOTORESISTOR PO SENSOR.

| PO Sensor | | | | | | | |
|---|---|---|---|---|---|---|---|
| LED-photoresistor | | | | LED-phototransistor | | | |
| 0.7mm | | 0.2 mm | | 0.7mm | | 0.2 mm | |
| d= 78mm | d= 113mm | d= 78mm | d= 113mm | d= 69.4mm | d= 122mm | d= 78mm | d= 113mm |
| 1.66 | 0.87 | 5.35 | 2.63 | 1.48 | 0.59 | 2.37 | 0.59 |

In Fig. 11, it can be noticed that the relative angular sensitivity reaches the maximum values in the measurement domain central area of the PO sensor, in the case of LED-phototransistor PO sensor, and in its neighbourhood, in the case of the LED-photoresistor PO sensor. This maximum point corresponds to the inflexion point of function $I=I(\alpha)_{d=const.}$, (1). The value of angle ($\alpha_i$), corresponding to the inflexion point can be calculated according to (8), [8], as follows,

$$tg\alpha_i = \frac{1}{\sqrt{2a-1}} \quad (8)$$

In the case of the LED-phototransistor PO sensors fitted with 0.7 mm Polaroid filters, the inflexion point corresponding to a = 1 (Table I) is $\alpha_i$ = 45°.

As parameter (a) decreases (Table I), PO sensor characteristics in Fig. 11 are moving to right, their shape becoming even asymmetric in the case of the LED-photoresistor PO sensor fitted with 0.2 mm filters.

These features make the PO LED-phototransistor be preferred when designing PO sensors with distance adjustment.

In Fig. 12, there are represented the characteristics $S_{\alpha r} = S_{\alpha r}(d)_{\alpha=const.}$ of LED-phototransistor and LED-photoresistor PO sensors, for 0.2 mm and 0.7 mm filters. These characteristics show the dependence of the relative angular sensitivity on the distance (d) between modules ($T_x$) and ($R_x$), when angle ($\alpha$) is constant.

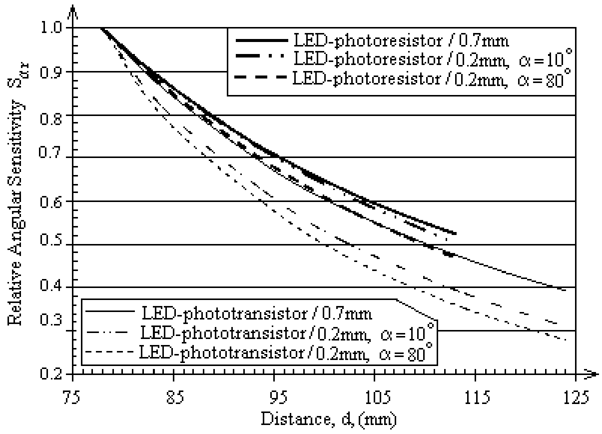


Fig. 12. Graphical representation of the characteristics $S_{\alpha r} = S_{\alpha r}(d)_{\alpha=const.}$ of the LED–phototransistor and LED–photoresistor PO sensor, (3).

From Fig. 12, it can be noticed that, in the case of the relatively intense lighting (for 0.2 mm Polaroid filters), the positions of the characteristics $S_{\alpha r} = S_{\alpha r}(d)_{\alpha=const.}$ depend on angle ($\alpha$). This feature must be taken into account when the PO sensor distance adjustment is used, in practice. For instance, if the sensor LED gets old, this one can be re-calibrated by modifying the distance between modules ($T_x$) and ($R_x$). If re-calibration is performed by using 0.2 mm filters, for sensor adjustment one must consider angle ($\alpha$), made of the polarizing plans of the Polaroid filters. This problem does not appear in the case of 0.7 mm filters.

Relation (3) allows the design of an intelligent transducer, which can automatically re-calibrate the PO sensor, when LED ageing occurs, as well as with the emission of a warning signal, when the LED is too much deteriorated.

When the PO sensor measures linear displacements and the adjustment is angular, one must know the device characteristics $S_{dr}= S_{dr}(\alpha)_{d=const}$ and $S_{dr}= S_{dr}(\alpha)_{d=const.}$.

Fig. 13 presents the characteristics $S_{dr}= S_{dr}(\alpha)_{d=const}$ of the two types of PO sensors, for 0.2 mm şi 0.7 mm polarizing filters. These characteristics show the dependence of the relative linear sensitivity on angle ($\alpha$), when the distance between modules ($T_x$) and ($R_x$) is constant.

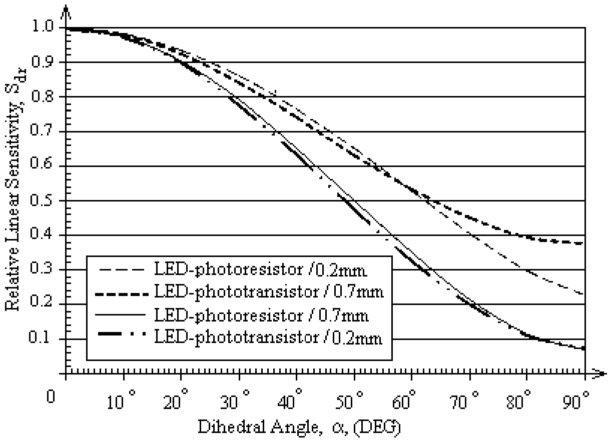


Fig. 13. Graphical representation of the characteristics $S_{dr}= S_{dr}(\alpha)_{d=const.}$ of the LED–phototransistor and LED–photoresistor PO sensor, (4) and (5).

The maximum values expressed in (μA/mm) of the PO sensors linear sensitivity absolute value corresponding to the extreme values of distance (d), are presented in Table III.

TABLE III. THE MAXIMUM VALUES EXPRESSED IN (μA/mm) OF THE ABSOLUTE VALUE'S LINEAR SENSITIVITY OF THE LED-PHOTOTRANSISTOR AND LED-PHOTORESISTOR PO SENSOR.

| PO Sensor | | | | | | | |
|---|---|---|---|---|---|---|---|
| LED-photoresistor | | | | LED-phototransistor | | | |
| 0.7 mm | | 0.2 mm | | 0.7 mm | | 0.2 mm | |
| d= 78 mm | d= 113 mm | d= 78 mm | d= 113 mm | d= 78mm | d= 124 mm | d= 78 mm | d= 113 mm |
| 2.36 | 0.86 | 9.89 | 3.85 | 3.49 | 0.87 | 11.03 | 2.42 |

In this case, the differences between the values of the relative linear sensitivity as a result of the (a) parameter variations at relatively intense lighting (the 0.2 mm Polaroid filters) are negligible.

In Fig. 13, it can be noticed that the relative linear sensitivity presents the smallest variation on the angular measurement domain for LED-phototransistor PO sensor fitted with 0.7 mm Polaroid filters. This characteristic confers the LED-phototransistor PO sensor a supplementary advantage as compared with the LED-photoresistor PO sensor.

Fig. 14 presents the characteristics $S_{dr}= S_{dr}(d)_{\alpha=const.}$ of the LED-phototransistor and LED-photoresistor PO sensors. These characteristics show the dependence of the relative linear sensitivity on distance (d) between modules ($T_x$) and ($R_x$), when angle (α) is constant.

From Figures 12 and 14, we can notice that the relative linear and angular sensitivities have maximum values if distance (d) between modules ($T_x$) and ($R_x$) is minimum.

In case 0.7 mm filters use, the differences appearing between the characteristics $S_{dr}= S_{dr}(d)_{\alpha=const.}$ of the LED–phototransistor and LED–photoresistor PO sensor, are not so big as to impose the use of one of the two devices.

As the characteristics $I = I(\alpha)_{d=const.}$ and $I = I(d)_{\alpha=const.}$ of PO sensors are non-linear, their linearization is to be made by the signal conditioning circuit. This process can be performed both digitally by and analogically, [9]-[12].

PO sensors can also be used without the signal linearization circuit, if they are designed to function in the area where the linearity of the static characteristics is good enough. When the PO sensor is used to measure the angles, a LED-phototransistor PO sensor with 0.7 mm Polaroid filters is recommended, as the inflexion point of its characteristics $I = I(\alpha)_{d=const.}$, corresponds to the centre of the measurement domain, $\alpha_i = 45°$.

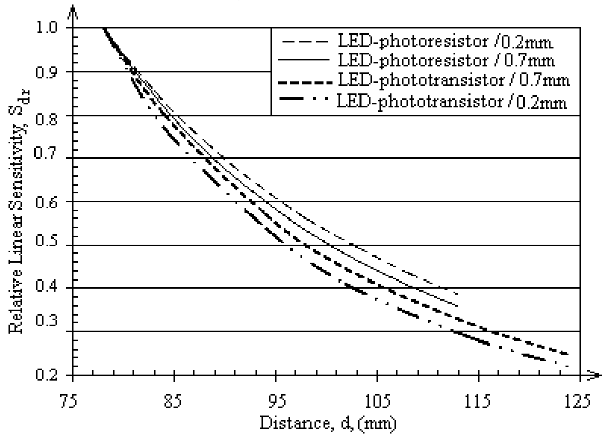


Fig. 14. Graphical representation of the characteristics $S_{dr} = S_{dr}(d)_{\alpha=const.}$ of the LED–phototransistor and LED–photoresistor PO sensor, (4) and (5).

If this sensor is designed to function in the measurement domain 20°≤ α ≤70°, the relative error of no-linearity is (Fig. 15):

$$\varepsilon_n = \frac{\Delta y_{max.}}{y_{max.78mm} - y_{min.78mm}} = \frac{1.18\mu A}{81.0\mu A - 14.1\mu A} = 1.77\% \quad (9)$$

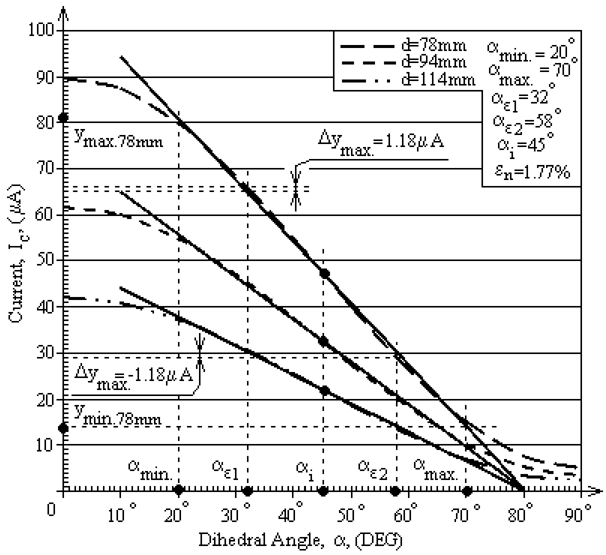


Fig. 15. Graphical representation of the linearity area of the characteristics $I_C = I_C(\alpha)_{d=const.}$ of the LED–phototransistor PO sensor.

The equations of the lines approximating characteristics $I_C = I_C(\alpha)_{d=const.}$ have been obtained by the method of least squares. In the case of the characteristic $I_C = I_C(\alpha)_{d=78mm.}$ the equation has the following form:

$$I_{C,d=78mm} = A + B \cdot \alpha = 107.6\mu A - 1.33\frac{\mu A}{DEG} \cdot \alpha \qquad (10)$$

Although the calculation of the relative error of non-linearity has been made in the case when d = 78 mm, ($\varepsilon_n$) has the same value for the whole family of static characteristics $I_C = I_C(\alpha)_{d=const.}$.

In Fig. 15, $\alpha_{\varepsilon1}$ and $\alpha_{\varepsilon2}$ are the angles for which the absolute error of non-linearity is maximum. Angles $\alpha_{\varepsilon1}$ and $\alpha_{\varepsilon2}$ have the same value for the whole family of static characteristics $I_C = I_C(\alpha)_{d=const.}$.

PO sensors are devices which do not present hysteresis. If the signal generated by a PO sensor is applied to a Schmitt trigger circuit one obtains a mechanical-electrical optoisolator transducer with hysteresis. This transducer can memorize two distinct values of the input quantity, its aim being to emit two distinct notice signals (the case of the level sensors of the liquid tanks) [13].

The angular ($d\alpha$) and linear (dd) sensitivity thresholds of the two types of PO sensors are: $d\alpha < 0.25°$ and dd < 0.24 mm.

These thresholds produce an angular resolution $(dI_C)_\alpha < 0.33\ \mu A$ and a linear resolution $(dI_C)_d < 0.6\ \mu A$ in the central area of the characteristics $I_C = I_C(\alpha,d)$ of the LED-phototransistor/0.7 mm PO sensor.

Unlike digital optical encoders, where the optical disk limits the minimum value of the angular sensitivity threshold as well as the device resolution, the Polaroid filters of the PO sensors, practically do not introduce such thresholds. The threshold of angular sensitivity ($d\alpha$) of digital optical encoders is $d\alpha < 0.5°$.

As for the PO sensors, the thresholds minimum values are mainly imposed by the characteristics of the mechanic system (mechanic frictions and the play in the mechanic device).

The sources of internal noise encountered at the PO sensor are located in the LED, in the photosensitive element and can be caused by optical and mechanic couplings.

The noise experiments performed on optocouplers with phototransistor of TIL112 and CNY 17 types, showed that the intensity of the LED noise and the noise of the optical channel does not influence an optocoupler output noise. The noise properties of the optocoupler device in a low frequency range depend on the noise sources existing in the phototransistor. The TIL112 and CNY 17 optocouplers consist in a Gallium Arsenide infrared emitting diode, optically coupled to a silicon NPN phototransistor. These optocouplers noise intensity is smaller than the angular and linear resolutions of the LED-phototransistor/0.7 mm PO sensor [14]-[16].

## V. Conclusions

LED-phototransistor and LED-photoresistor PO sensors are analogue optoelectronic devices, which allow the change of rotation and/or translation movements into electrical signals.

The PO sensors transfer static characteristics are non-linear. Their non-linearity is caused by the non-linear dependence of the luminous lighting ($E_v$) of the photoelement on the distance (d) between modules ($T_x$) and ($R_x$) and on the angle between the Polaroid filters polarizing plans ($\alpha$).

In order to compare LED-phototransistor and LED-photoresistor PO sensors, we graphically represented the dependences of the relative angular ($S_{\alpha r}$) and linear ($S_{dr}$) sensitivities of the ($\alpha$) angle sensors between the Polaroid filters polarizing plans and the distance (d) between modules ($T_x$) and ($R_x$).

These representations showed that the form of the characteristics $S_{dr} = S_{dr}(d)_{\alpha=const.}$ şi $S_{\alpha r} = S_{\alpha r}(\alpha)_{d=const.}$ depends on the form of the light characteristics $I = I(E_v)_{V=const.}$ of the photosensitive elements by means of parameter (a).

The smaller the parameter (a) variations are, as its value is closer to a = 1, the better the linearity of the characteristics $I = I(\alpha)_{d=const.}$ on the interval $20° \le \alpha \le 70°$, the relative error of non-linearity being smaller.

This condition is best accomplished by the LED-phototransistor sensor fitted with 0.7 mm wide Polaroid filters.

The use of Polaroid filters does not limit the minimum value of the angular sensitivity threshold. This characteristic allows obtaining some PO sensors with dimensions which are smaller than those of the digital optical encoders and with a lower sensitivity threshold.

The distance adjustment of the PO sensor allows their re-calibration in time, once with the LED ageing.

## Acknowledgment

This work was partially supported by European Framework Program 7 under the contract no. PIRG02-GA-2007-224904.

## References

[1] L. Vladareanu, G. Tont, I. Ion, M. S. Munteanu and D. Mitroi, “Walking Robots Dynamic Control Systems on an Uneven Terrain”, Advances in Electrical and Computer Engineering, vol.10, no.2, pp. 145-152, 2010.

[2] M. Y. Usher, Sensors and Transducers, Mac-Millan Published, London, GB, 1985.

[3] G. Raţă, M. Raţă, I. Graur and D. L. Milici, “Induction Motor Speed Estimator Using Rotor Slot Harmonics”, Advances in Electrical and Computer Engineering, vol. 9, no. 1, pp. 70-73, 2009.

[4] A. Malik, M. Aceves and S. Alcantara, “Novel FTO/SRO/silicon optical sensors: characterization and applications” IEE Proc. Sensors, vol. 1, pp. 116-120, Nov. 2002.

[5] I. M. Ciuruş, “Optocuplor polaroid” (patent pending), OSIM Bucureşti, RO, a2009 00270, 2009.

[6] I. M. Ciuruş, M. Dimian and A. Graur, “Mechanical-electrical Optoisolator Transducer with current-to-frequency conversion”, Proc. 10th Int. Conf. Development and Application Systems, Suceava, RO, May 2010, pp. 119-124.

[7] I. M. Ciuruş, M. Dimian and A. Graur, “Mechanical-electrical Optoisolator Transducers”, Proc. IEEE 12th Intern. Conf. Optimization of Electrical and Electronic Equipment, Braşov, RO, May 2010, pp. 740-745.

[8] I. M. Ciuruş, M. Dimian and A, Graur, “LED-photoresistor Mechanical-electrical Optoisolator Transducers”, Journal of Optoelectronics and Advanced Materials, Submitted for publication.

[9] J. M. D. Pereira, O. Postolache and P. M. B. S. Girao, “PDF-Based Progressive Polynomial Calibration Method for Smart Sensors Linearization”, IEEE Trans. Instrumentation and Measurement, vol.58, pp. 3245-3252, Aug. 2009.

[10] R. G. Bozomitu, V. Cehan and V. Popa, “A New Linearization Technique Using “Multi-sinh” Doublet”, Advances in Electrical and Computer Engineering, vol. 9, no. 2, pp. 45-57, 2009.

[11] M. P. Kraska, “Digital linearization and display of non-linear analog (sensor) signals”, IEEE Workshop Automotive Applications of Electronics, Dearborn, US, 1988, pp. 45-51.

[12] M. Ciugudean, V. Tiponuţ, M. E. Tănase, I. Bogdanov, H. Cârstea and A. Filip, Circuite integrate liniare. Aplicaţii, Editura Facla, Timişoara, RO, 1986, ch. 2, sec. 2.5, pp.58-64.

[13] I. M. Ciuruş, M. Dimian and A. Graur, “Mechano-electric Optoisolator Transducer with Hysteresis”, 5th Int. Workshop Multi-rate Processe & Hysteresis in Mathematics, Physics, Engineering and Information Sciences, Pécs, HU, May/June 2010, pag. 8.

[14] M. M. Jevtić, “Low frequency noise as a tool to study optocouplers with phototransistors”, Microelectronics Reliability, vol. 44, pp. 1123-1129, May 2004.

[15] A. Konczakowska, J. Cichosz, A. Szewczyk and B. Stawarz, “Analysis of noise properties of an optocoupler device”, Opto-Electronics Review, vol. 15, pp. 149-153, Sept. 2007.

[16] A. Konczakowska, J. Cichosz, A. Szewczyk and B. Stawarz, “Identification of optocoupler devices with RTS noise”, Fluctuation and Noise Letters, vol. 6, pp. L325-L404, Sept. 2006.